

Determining Relaxation Modes in Flowing Associative Polymers Using Superposition Flows

J. Mewis,* B. Kaffashi,[†] and J. Vermant

Department of Chemical Engineering, K.U. Leuven, W. de Croylaan 46, B-3001 Leuven, Belgium

R. J. Butera

Dupont Performance Coatings, Marshall Research and Development Laboratories, 3401 Grays Ferry Avenue, Philadelphia, Pennsylvania 19416

Received June 6, 2000; Revised Manuscript Received November 15, 2000

ABSTRACT: Oscillations superimposed on steady shear flows have been used repeatedly in the past to determine the relaxation modes in flowing associative polymers. In these experiments, the oscillatory motion has been parallel to the steady-state flow. Here, parallel superposition moduli on associative polymers will be compared with superposition experiments in which the oscillatory motion is perpendicular to the steady-state flow. In the latter experiments, there is less interference between the steady flow and the superimposed oscillations, which has drastic consequences for the results. Data are shown for a HASE polymer (hydrophobic alkali-swellaable emulsion). As in other fluids, the limiting viscosities at zero frequency differ drastically, and negative storage moduli can be obtained in parallel superposition. The apparent relaxation frequencies during flow, as derived from parallel superposition measurements, are an order of magnitude smaller than those derived from orthogonal superposition. The effect of shear rate on the average relaxation times seems to be qualitatively similar in the two superposition modes, but the moduli–frequency curves differ in shape. The shapes of these curves also reflect the associative nature of the polymers.

1. Introduction

In associative polymers, nonchemical bonds develop between the molecules. These bonds cause the formation of a supermolecular structure that varies according to the flow conditions to which the material is subjected. As a result, these materials display a very complex rheological behavior. The main interest, both industrially and scientifically, has been in hydrophobically modified, water-soluble polymers. In such systems, the hydrophobic groups have a tendency to cluster together, which can lead to associations between two or more polymer chains. The present views on their rheology and microstructure have been reviewed recently.¹

The associating groups can be positioned in various ways along the polymer chain. In the simplest case, that of telechelic polymers, the groups are attached at the ends of linear chains (ABA structure). In aqueous media, hydrophobic ethoxylated urethanes (HEURs) have been used to generate telechelic polymers, although the same groups can be incorporated into more complex structures as well. Under suitable conditions, both hydrophobic ends of several telechelic HEUR molecules will cluster together, producing flowerlike micelles. These can, in turn, aggregate into strings or networks of micelles by means of molecules having their end groups in different micelles.^{2–4} In such systems, relaxation proceeds by retraction of the telechelic molecules from a micelle. As a result, the relaxation behavior is characterized by a single relaxation time.⁵ This type of response is somewhat similar to that of wormlike micelles that are formed in surfactant solutions.⁶ Transient network theories have been applied to the rheology of associative polymers.^{5,7–9}

The hydrophobic groups can also be distributed along the polymer chain rather than being attached at the ends. This has been achieved in HEURs as well as in hydrophobic alkali-swellaable emulsions (HASE). The latter behave as latex emulsions at low pH but develop into associative polymer solutions in alkaline media. The presence of hydrophobic groups at several places along the chain results in a more complex structure and rheology, as a result of the changing balance between intra- and intermolecular hydrophobic links.^{10–12} The viscosity curves of associative polymers often include a shear-thickening region at intermediate shear rates.^{5,13} The molecular aggregation that causes shear thickening shows up in transient experiments as well. The stress relaxation after cessation of flow, for instance, can evolve in a different and more complex manner than it does in ordinary polymer fluids.¹⁴ Not surprisingly the Cox–Merz analogy between the steady-state viscosities and the dynamic viscosities is not always satisfied.^{5,11,15}

In some commercial rheometers, it is now possible to perform superposition flows. Such rheometers have been used to study structural changes during flow in various systems, including polymeric fluids as well as colloidal suspensions.^{16–19} The changes in their supermolecular structure during flow make associative polymers also very suitable for being studied in this manner.^{11,12,15,20} In these investigations, it has been assumed that superposition flows can be analyzed as ordinary linear oscillatory flows. This assumption is not necessarily correct, as is known from work on other polymers.^{21,22} The validity of this approach for associative polymers will be evaluated here.

2. Superposition Techniques in Rheology

Rheological superposition measurements belong to a general class of physical techniques in which nonlinear

* Author to whom correspondence should be addressed.

[†] Present address: Department of Chemical Engineering, University of Tehran, Engelab Ave, Tehran, Iran.

phenomena are studied by means of linear perturbation analysis. In rheology, one deals with nonlinear dynamic systems, the relevant parameters of which are tensorial in nature. This requires a mathematical framework for which no useful general scheme is available. Earlier studies on associative polymers seem to have treated the data in the same manner as those from oscillatory flow without superimposed steady shearing flow. The software provided by the manufacturers of commercial rheometers has been based on the same approach. In superposition studies on other materials, the Yamamoto analysis has often been used.²³ The latter author started from an integral Lodge model and allocated to each deformation rate, characterized by the second invariant of the rate of deformation tensor I_{2D} , a perturbation spectrum $H(\tau, I_{2D})$, with τ the relaxation time. For the case of simple shear flow, the second invariant reduces to $\dot{\gamma}^2$, with $\dot{\gamma}$ the shear rate. When using $H(\tau, I_{2D})$, it is implicitly assumed that the rate of strain is the governing kinematic parameter that is being perturbed linearly by the small amplitude oscillatory flow. Hence, the superposition flow is described by

$$\sigma = \int_{-\infty}^t \left[\int_{-\infty}^{\infty} \frac{H(\tau, I_{2D})}{\tau} \exp\left(-\frac{(t-t')}{\tau}\right) d \ln \tau \right] (\mathbf{C}^{-1} - \mathbf{I}) dt' \quad (1)$$

where \mathbf{C}^{-1} is the Finger strain tensor.

Equation 1 has been suggested not as a generally applicable constitutive equation but only to describe superposition flows. The resulting relation between oscillatory stress and strain depends on the relative orientation between the steady-state shear flow and the oscillatory flow. Indeed, two types of superposition flows have to be distinguished. With 1 being the direction of the velocity and 2 that of the velocity gradient of the steady-state shear flow, the steady-state flow generates a nonzero 12-component of the strain rate tensor. The velocity and velocity gradient of the superimposed oscillation can then be parallel to those of the stationary flow, providing an additional contribution to the component $\dot{\gamma}_{12}$. Alternatively, a periodic $\dot{\gamma}_{13}$ can be applied by oscillation in the vorticity direction (3-direction); this is called orthogonal superposition.¹⁶ Parallel superposition flow is now available on several commercial, stress-controlled rheometers. Orthogonal superposition has been used less frequently,^{16–18,21} although a possible setup, based on a modification of a commercial device, has been described recently.²⁴

The Yamamoto analysis predicts a totally different behavior for the two superposition modes. It turns out that, in the parallel variety, the stationary and oscillatory flows are strongly coupled, which results in complex expressions for the superposition moduli^{21,23}

$$G_{\parallel}(\omega, \dot{\gamma}) = \int_{-\infty}^{\infty} \left[H(\tau, \dot{\gamma}^2) + 4\dot{\gamma}^2 \frac{\partial H(\tau, \dot{\gamma}^2)}{\partial \dot{\gamma}^2} \frac{1}{1 + \omega^2 \tau^2} \right] \frac{(\omega \tau)^2}{1 + \omega^2 \tau^2} d \ln \tau \quad (2)$$

$$G_{\perp}(\omega, \dot{\gamma}) = \int_{-\infty}^{\infty} \left[H(\tau, \dot{\gamma}^2) + 2\dot{\gamma}^2 \frac{\partial H(\tau, \dot{\gamma}^2)}{\partial \dot{\gamma}^2} \frac{1 - \omega^2 \tau^2}{1 + \omega^2 \tau^2} \right] \frac{\omega \tau^2}{1 + \omega^2 \tau^2} d \ln \tau \quad (3)$$

with ω the frequency of the oscillatory mode. These equations indicate that the parallel superposition moduli at a given shear rate are not only determined by the corresponding perturbation spectrum $H(\tau, \dot{\gamma}^2)$ but also by its change with shear rate. The expressions for the orthogonal superposition moduli, according to the Yamamoto analysis, are given by equations similar to the parallel ones, except that the terms containing the derivative of H no longer appear. Hence, the equations reduce to those of the linear theory of viscoelasticity, but now using a shear-rate-dependent spectrum rather than the linear one. According to this analysis the superposition spectrum can be calculated from the orthogonal superposition moduli by means of the relations derived from the linear theory of viscoelasticity. For the parallel superposition moduli from eqs 2 and 3, this is clearly not the case. Also, the two parallel superposition moduli are not interrelated by the Kramers–Kronig relation, as should be the case for linear dynamic systems. In fact, as the perturbation spectra normally decrease with increasing shear rate, the parallel superposition moduli, in particular G_{\parallel} , can even become negative. This has actually been verified for ordinary polymer solutions.^{21,25} The expressions for the orthogonal superposition moduli, resulting from the same analysis, do not produce negative values for the moduli. In addition, the zero frequency dynamic viscosity in orthogonal superposition reduces to the steady-state viscosity at the applied shear rate, which is not the case for the parallel superposition.

It has been demonstrated that the use of a shear-rate-based perturbation spectrum, as discussed above, does not necessarily provide a sufficiently general basis for analyzing superposition flows.²¹ This can be seen by using nonlinear viscoelastic models such as the integral Wagner model, which provides analytical solutions for the superposition flows. Such a model does not necessarily hold for associative polymers, but the available theoretical and experimental results clearly indicate that treating parallel superposition moduli as simple linear moduli is not generally valid.^{21,26–28}

3. Experimental Section

A system (TT-615 from Rohm & Haas) has been selected that could be measured quite accurately with the available orthogonal superposition device. It contains acrylic acid and methylmethacrylic groups, as well as ethylene oxide spacers to which the hydrophobic groups are attached. It can be classified as a branched HASE system. It was received in latex form at a concentration of 32% w/w. Dilutions were prepared using deionized, twice-distilled water; these were then solubilized by adding gradually a 1 N NaOH solution with stirring until the pH reached ca. 8.9.

The parallel superposition measurements were performed on a stress-controlled rheometer (DSR from Rheometric Scientific). Cone-and-plate geometries were used with different radii (25 and 40 mm) and different cone angles (0.1 and 0.04 rad). The two cone angles produced similar viscosity curves. This indicates that slip is not a major issue. A solvent trap was used to avoid evaporation of the water.

For the orthogonal superposition measurements, an RMS800 rheometer (Rheometric Scientific) was modified. By feeding an oscillatory signal into the feedback loop of a force rebalance transducer, a periodic axial motion can be applied to a sample that is being sheared continuously in the tangential direction. The sample is contained in a specially designed double Couette cell, executed so as to avoid a pumping motion in the fluid. The details, as well as the procedures for measuring and calculating the orthogonal moduli, have been published elsewhere.²⁴

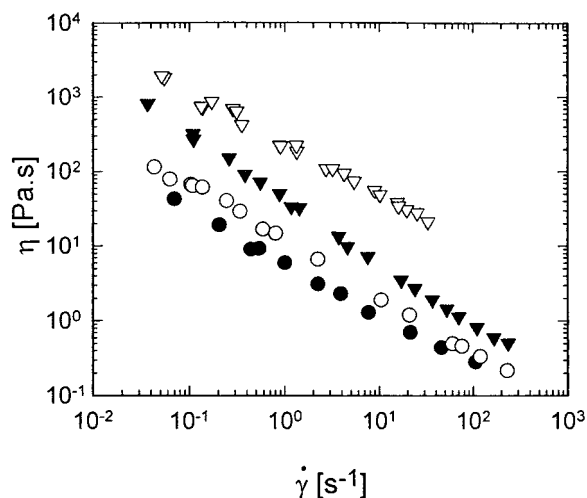


Figure 1. Viscosity functions for four different concentrations (w/w) of a HASE associative polymer: ●, 0.7%; ○, 1.0%; ▼, 1.2%; ▽, 1.9% ($T = 25.0\text{ }^{\circ}\text{C}$).

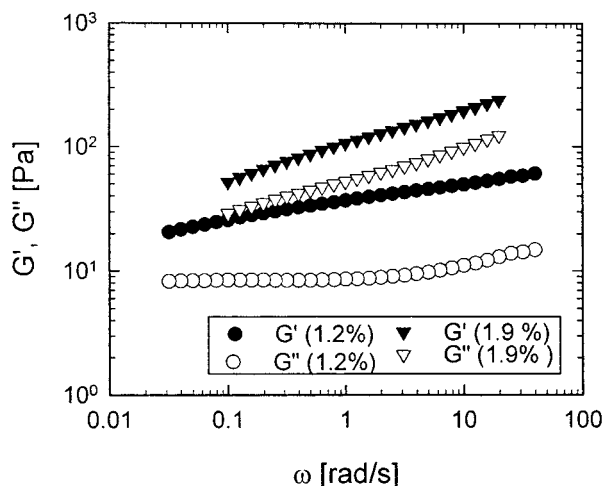


Figure 2. Storage and loss moduli at rest for two concentrations of associative polymer ($T = 25.0\text{ }^{\circ}\text{C}$).

4. Results and Discussion

4.1. Steady-State Viscosities and Linear Moduli.

The viscosity curves $\eta(\dot{\gamma})$ at the polymer concentrations under consideration, Figure 1, do not contain a Newtonian region in the range of shear rates covered here. The pronounced shear thinning suggests a highly structured system that breaks down progressively with increasing shear rate. No shear-thickening zone could be detected. The curves for different polymer concentrations are not completely parallel. At intermediate concentrations, the low shear viscosities increase slightly more with concentration than at high shear rates. This effect disappears at higher concentrations. Such a different concentration dependence for low and high shear viscosities is not uncommon for associative polymers.^{13,29} Otherwise, the viscosity curves of Figure 1 do not explicitly indicate any associative effect in the polymers.

With the linear dynamic moduli (Figure 2), the equilibrium structure of the samples can be probed. In associative polymers the equilibrium structure will not be recovered instantaneously after the flow is stopped. By following the evolution of the moduli as a function of time, it has been verified that any flow-induced changes in structure were fully decayed before G' and

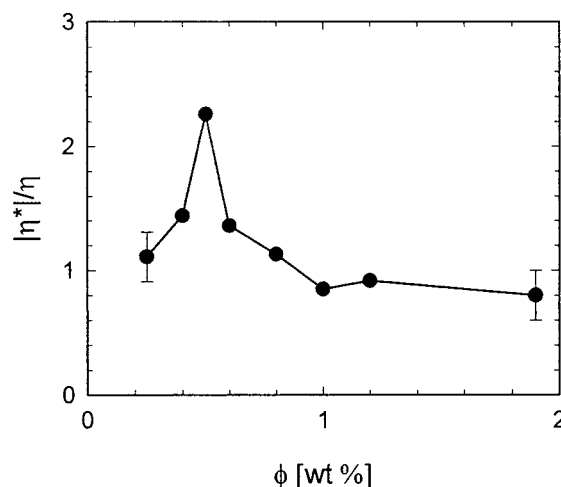


Figure 3. Ratio of the dynamic to the steady-state viscosity at 0.1 s^{-1} .

G'' (storage and loss moduli, respectively), were measured as a function of frequency. The data in Figure 2 reflect such equilibrium conditions. The dynamic behavior is not Maxwellian, contrary to what is observed in telechelic associative polymers. HASE polymers are known to show a wide distribution of relaxation times.^{10–12} In the low-frequency regime, no terminal zone (i.e., G' proportional to ω^2 and G'' proportional to ω) could be detected. Yet, the loss tangent ($\tan \delta = G''/G'$) increases with decreasing frequency, indicating that the available frequency range does not cover all relaxation modes and that a terminal zone might appear at still lower frequencies. Time–temperature superposition cannot be applied to extend the frequency range as the intermolecular structure is expected to change with temperature. The lack of a terminal zone at low frequencies could be consistent with the lack of a Newtonian region in the steady-state viscosity curves. Also, the fact that the storage moduli are higher than the loss moduli confirms that some degree of long-range structure, having smaller relaxation frequencies, is present in the material. A finite but large limiting relaxation time is expected for gels with physical links that have a nonzero probability of breaking. This could be the case here.

Associative polymers often display a characteristic shear-thickening region at intermediate shear rates.^{5,13,15} Such a region is not observed here (Figure 1). Data at lower concentrations, available as Supporting Information, also showed shear-thinning behavior over the entire shear rate range (available as Supporting Information). Another frequent feature of associative polymers is that they do not obey the Cox–Merz analogy between the magnitude of the dynamic viscosity ($|\eta^*|$) and the steady-state viscosity (η). More specifically, the ratio $|\eta^*|/\eta$ is smaller than unity.^{15,20} This viscosity ratio is shown in Figure 3 as a function of concentration at a shear rate of 0.1 s^{-1} . At this shear rate, a shear-thinning behavior was observed for all concentrations under consideration. The value of the ratio shows a maximum at approximately 0.5 wt %. The ratio drifts below unity at concentrations of 1% and above. The data at other frequencies and shear rates follow the same general trend. Associative polymers typically do not display values of this viscosity ratio greater than unity, contrary to what has been observed for colloidal suspensions.³⁰

Based on the above observations, the question arises whether the systems under consideration behave as

associative polymers or whether residual gel particles are responsible for the rheological response. Associative polymers can indeed contain microgel particles, which in some cases seem to dominate the rheological behavior.²⁰

Shear thickening in associative polymers is usually attributed to either a flow-induced change from intramolecular to intermolecular associations³¹ or a flow-induced non-Gaussian stretching of the chains.⁹ Experimental evidence for the latter has been presented recently.¹⁴ These structural changes would also explain the deviations from the Cox–Merz rule that are normally exhibited by associative polymers. The complicated concentration dependence of the Cox–Merz relationship represented by Figure 3 could be rationalized if some fraction of the polymer were present as microgel particles. A small amount of polymer, present as swollen microgel particles, could account for a substantial rise in viscosity. The strong shear-thinning behavior caused by even small concentrations of these particles would likely mask any residual shear thickening from the free associative polymer or from associations between the microgel particles. This would also cause the characteristic high values of $|\eta^*|/\eta$ mentioned above. If these materials were composed of simple microgel particles with no associative character, η would be expected to be lower than $|\eta^*|$ at all concentrations at moderate shear rates. The reverse would hold at very high shear rates.

It is possible to obtain evidence for intermolecular association by examining the strain dependence of the moduli. The data in Figure 2 were obtained at sufficiently small strains to be in the linear region. Increasing the strain will result in nonlinearities that are different for the different types of materials. For simple polymer solutions, both moduli will decrease with strain, with G' producing the strongest decrease. In concentrated suspensions, G' can initially increase; at somewhat larger strains, G' starts to decrease, and it requires still larger strains for G'' to decrease as well. With associative polymers, the molecules can be stretched before the intermolecular links break down. As a result, the storage moduli initially increase with strain.^{11,15} In some systems with associative polymers, no strain hardening occurs,²⁰ which can be attributed to the polymer being present as microgel particles.

In the present case, strain hardening can be observed at intermediate strains, followed by a systematic breakdown at higher strains (Figure 4). Both moduli increase, and hence, the structural change induced by strain also increases the dissipative part G'' . The elastic part, G' , increases less than the viscous one and starts to decrease first. Such a strain dependence of G' and G'' has been reported previously for HASE associative polymers.^{11,15} It can be concluded that the measured strain dependence of the moduli reflects that of HASE systems. The materials investigated here could contain microgel particles. However, the strain dependence of the moduli and the complex deviation from the Cox–Merz relationship as a function of concentration suggest that there is a significant associative effect in this system, even in the absence of a shear-thickening regime.

4.2. Superposition Moduli. The parallel and orthogonal superposition measurements were performed on different instruments (see section 3). It is therefore imperative to verify that instrumental artifacts or

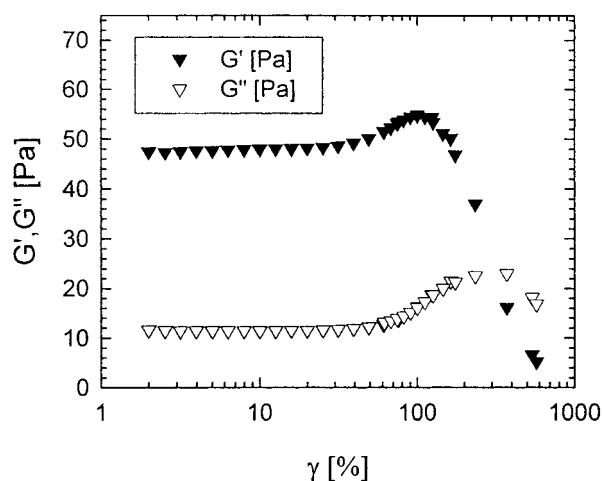


Figure 4. Strain dependence of storage (\blacktriangledown) and loss (\triangledown) moduli for a 1.2% solution of associative polymer, frequency = 10 rad/s.

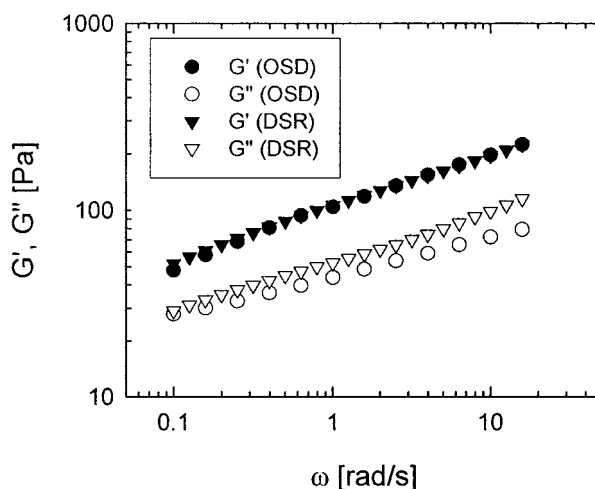


Figure 5. Comparison between the storage and loss moduli of a 1.9% solution of associative polymer, measured in a cone and plate rheometer (\triangledown , \blacktriangledown) and using the orthogonal superposition device (\circ , \bullet).

measurement conditions do not interfere with a comparison between the two types of results. The orthogonal superposition device (OSD) only operates at ambient temperature, introducing an additional source of uncertainty that should be evaluated. For that purpose the linear dynamic moduli, i.e., without any superposed steady-state flow, were determined on the two devices using the same sample. After the decay of all shear history effects, the samples should be isotropic and should produce identical results in the two experiments. The data (Figure 5) from the two instruments are quite similar. Some differences can be noticed in G'' , probably caused by the lower accuracy of the orthogonal device, but they are minor with respect to the differences that will be reported between the two types of superposition flow. Hence, it can be concluded that valid comparisons can be made. The agreement between the results from the two instruments, which have different measurement geometries and loading procedures, is again an indication that flow-induced changes in structure can fully decay, as discussed above.

As far as the actual superposition measurements are concerned, the parallel superposition moduli, $G_{||}^*$, will be considered first. The results (Figure 6) on a 1.2% sample are comparable with published data on HASE

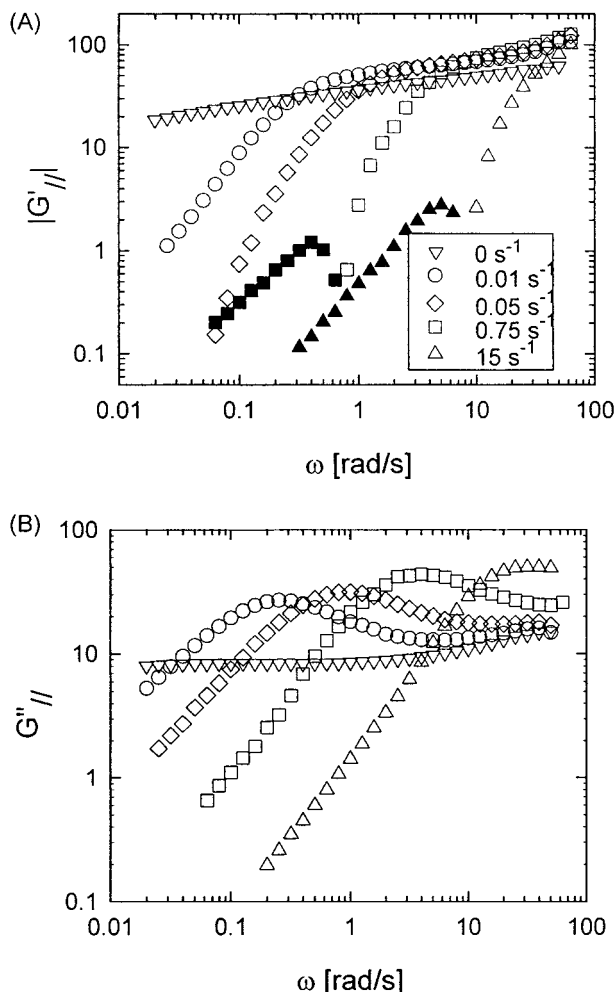


Figure 6. Parallel superposition moduli at different shear rates for the 1.2% sample: (A) in-phase components (open symbols, positive values; solid symbols, negative values); (B) out-of-phase components.

systems.^{11,12,15,20} Data were also obtained at other concentrations, with qualitatively the same behavior displayed. The main difference with ordinary polymer solutions is that the latter do not show an increase in the moduli at high or intermediate frequencies. Nonlinear viscoelastic models do not seem to produce such an increase either. In shear-thinning colloidal suspensions, a small increase in G' but not in G'' has been reported for parallel³² and orthogonal superposition.¹⁸ The associative polymer, therefore, seems to produce a specific superposition behavior, at least in parallel superposition.

The out-of-phase components, $G''_{||}$, become proportional to the frequency in the low-frequency region, at least for sufficiently large shear rates. Under such conditions, a limiting zero-frequency superposition viscosity can be determined. The corresponding in-phase components, $G'_{||}$, do not become proportional to ω^2 , as expected in the terminal zone in the case of linear viscoelastic behavior. They actually change more drastically with frequency and even drop below zero at still smaller frequencies, as is shown in Figure 6 (solid symbols). It is obvious that the parallel moduli cannot be discussed in the framework of linear viscoelasticity. The crossover frequency in particular, i.e., the point where $G'_{||} = G''_{||}$ has been used in the past to characterize the dominant relaxation frequency during flow.¹¹ This interpretation is derived from Maxwellian behavior

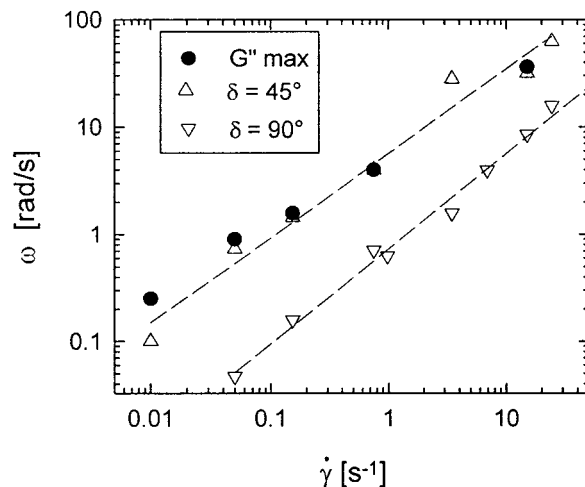


Figure 7. Evolution of the characteristic frequencies in parallel superposition as a function of shear rate for a 1.2% solution of associative polymer. Crossover frequency (Δ), frequency at which $G'_{||}$ changes sign (∇), and frequency at which $G'_{||}$ exhibits a maximum (\bullet).

and becomes questionable in cases such as those shown in Figure 6. The same conclusion can be drawn from calculations based on nonlinear viscoelastic models with multiple relaxation times.²¹

Because of the specific shape of the moduli–frequency curves, different characteristic frequencies can be defined in the case of parallel superposition (Figure 7). The first is the crossover frequency ($\delta = 45^\circ$), and the second is the frequency at which the curve of the loss moduli, $G''_{||}$, shows a maximum. In the framework of linear viscoelasticity, it would signify the presence of a dominant relaxation mode at that particular frequency. When the superposition moduli have negative values at low frequencies, the transition to positive values provides a third characteristic frequency. The latter is proportional to $\dot{\gamma}^{0.9}$ for the sample with 1.2% polymer, close to the value reported in the literature for nonassociating polymers.^{25,33} The crossover frequency shows a somewhat similar dependence on shear rate, possibly with a slightly smaller slope. Except perhaps at the smallest shear rates, the position of the maximum in $G''_{||}$ nearly coincides with the crossover frequency. In linear viscoelasticity, this is typical for Maxwellian fluids.

A 1.9% sample was used to compare the orthogonal superposition moduli with the parallel ones. In Figure 8, the in-phase and out-of-phase components of the moduli are given for the two types of superposition, using in each case a steady-state shear rate of 0.1 s^{-1} . Clearly the two data sets differ substantially. Only at the highest frequencies, where the effect of the superimposed steady shearing motion becomes smaller, do the two types of moduli seem to tend to similar values. Differences between the two superposition modes that decrease with increasing frequency are quite common. The characteristic increase in $G'_{||}$ at intermediate frequencies can also be detected in orthogonal superposition (see also later), but it is clearly less pronounced there. The net result is a large difference between the crossover frequency (ω_{co}) in the two superposition flows. In Figure 8, it can be seen that this frequency is an order of magnitude larger in parallel superposition than in the orthogonal mode.

In Figure 8, the two superposition modes have been compared at a single steady shear rate. The extent to

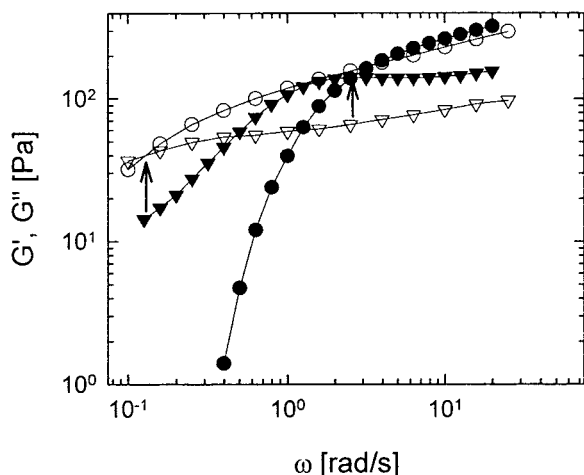


Figure 8. Comparison between the parallel (solid symbols) and the orthogonal superposition moduli (open symbols), for the sample with 1.9% (w/w) associative polymer, shear rate = 0.1 s^{-1} (\circ , G' ; ∇ , G'') (the arrows indicate the crossover frequencies).

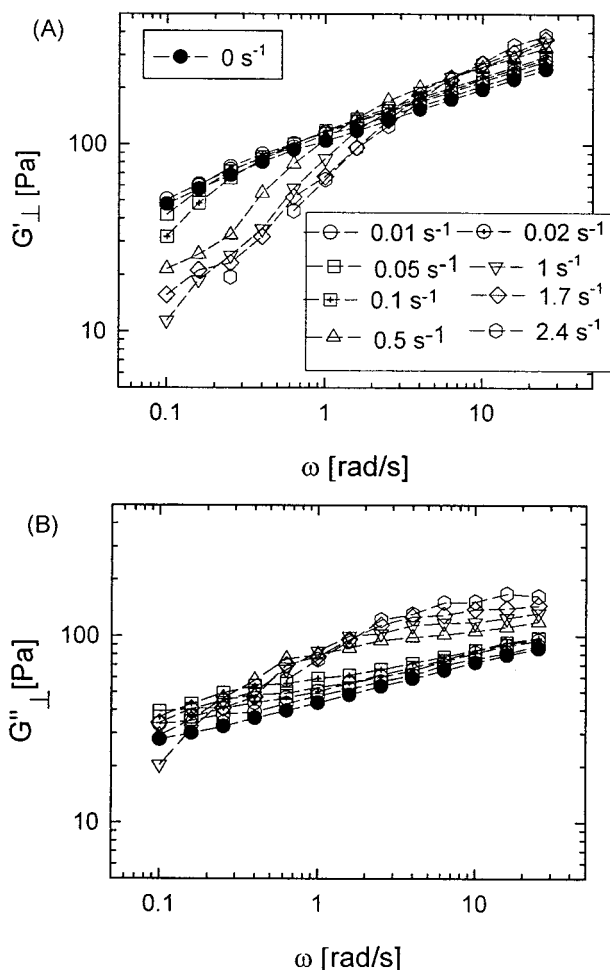


Figure 9. Evolution of the orthogonal superposition moduli with shear rate for the sample of Figure 8.

which the shear will affect the relation between the two types of moduli remains to be verified. The effect of shear rate on the orthogonal superposition moduli is illustrated for a 1.9% w/w sample in Figure 9, where a peak strain of 1.7% has been applied.

Common features as well as differences can be noticed when the two types of superposition moduli are compared. In the low-frequency range, all moduli decrease

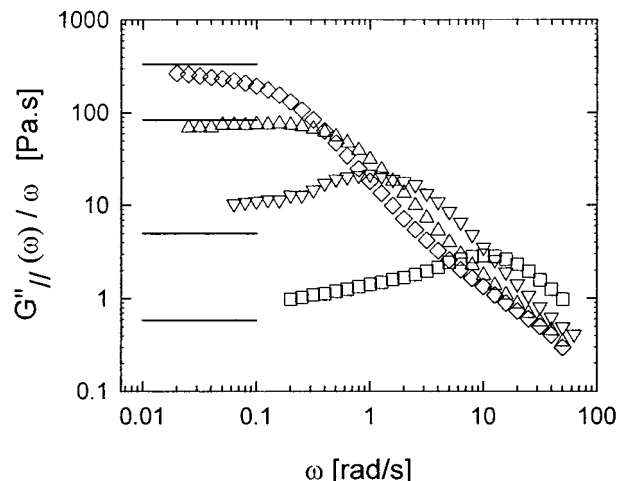


Figure 10. Comparison of the predictions of eq 4 using the viscosity data with the data of Figure 6.

with increasing shear rate. A similar behavior has been observed for other nonlinear systems during flow. Markovitz has derived relations between the limiting out-of-phase superposition moduli at zero frequency and the steady-state viscosities at the same shear rate.³⁴ These relations should hold quite generally for fluids with a fading memory. In the case of parallel superposition, the relation is given by

$$\lim_{\omega \rightarrow 0} \frac{G''_{||}(\omega, \dot{\gamma})}{\omega} = \eta(\dot{\gamma}) \left(1 + \frac{\partial \ln \eta(\dot{\gamma})}{\partial \ln \dot{\gamma}} \right) \quad (4)$$

For shear-thinning fluids, the steady-state viscosities decrease with shear rate. Equation 4 then predicts a limiting zero dynamic viscosity that is lower than the steady-state value. For orthogonal superposition the relation becomes

$$\lim_{\omega \rightarrow 0} \frac{G''_{\perp}(\omega, \dot{\gamma})}{\omega} = \eta(\dot{\gamma}) \quad (5)$$

In this case, the limiting dynamic viscosity becomes equal to the steady-state viscosity, as in linear viscoelasticity.

The data of Figure 6 are replotted in Figure 10 and compared with the limiting values derived from the steady-state viscosities of Figure 1 using eq 4. The zero limit is not always reached, but the data seem to agree within measuring accuracy with eq 4. For the orthogonal superposition mode, the data do not extend close enough to the terminal zone, and therefore, no direct comparison can be made with eq 5. Lower limits for the limiting viscosities can be estimated by extrapolating the experimental data of Figure 9. This produces values that are much larger than the parallel viscosities and that are close to the steady-state viscosities.

The effect of shear on the crossover frequency ω_{co} is compared for the two types of superposition in Figure 11. Over the shear rate range covered here, the orthogonal crossover frequency remains systematically smaller by an order of magnitude. For shear rates larger than 0.1 s^{-1} , the flow affects the crossover frequencies in the same manner. At lower shear rates, the two data sets might come closer together. The other characteristic frequencies have a nearly similar dependency on shear rate, as has been demonstrated in Figure 7 for the 1.2% sample. Although the parallel superposition measure-

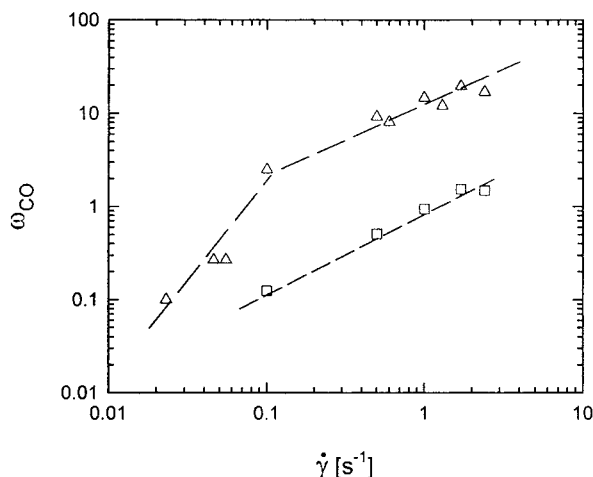


Figure 11. Comparison of the crossover frequencies in orthogonal (\square) and parallel (\triangle) superposition for the sample of Figure 8. The lines are provided to guide the eye.

ments do not reflect in a simple fashion the relaxation modes of the flowing system, the relative changes with shear rate are nevertheless quite similar in the two superposition modes. The extent to which this is a general result remains to be verified. The effect of shear rate also depends on concentration. At lower concentrations, the crossover frequency increases linearly with shear rate (Figure 7). In more concentrated solutions, the shear effect becomes less pronounced (Figure 11).

When characteristic relaxation times between the two superposition modes are compared, a problem similar to that with the zero shear viscosities arises. As at least the parallel superposition moduli do not obey the Kramers–Kronig relations, they cannot be translated directly in relaxation spectra. This can be illustrated by model calculations using the upper convected Maxwell model (see, e.g., Leonov et al.²⁶), a quasi-linear model with a constant relaxation time. This constant relaxation time does not describe the parallel superposition moduli at higher steady-state shear rates. Hence, it becomes more difficult to separate real nonlinearity from this quasi-linearity in such experiments.

The superposition data on associative polymers differ from those on other polymers by the increase with shear rate of the moduli at higher frequencies. Such behavior has also been reported for other parallel superposition measurements on similar materials.^{11,12,15,20} The global effect of shear on such systems could be explained by the destruction of long-range links, e.g., intermolecular or intermicellar, by flow. This enables the formation of additional short-range links, e.g., intramolecular or intramicellar, thus increasing the contribution from the relaxation modes at intermediate frequencies. The present results indicate that the same features also arise in orthogonal superposition flows and, therefore, are not caused by the specific coupling between the steady-state and parallel superposition flows. To deduce from the data, in particular from the parallel superposition experiments, quantitative information about the relaxation modes under shear is more complicated. The basic Kramers–Kronig relations no longer apply, as is amply demonstrated by the low-frequency moduli and viscosities in parallel superposition. Hence, relaxation times cannot be determined in the usual manner. Calculating the parallel superposition moduli for an upper convected Maxwell model (see, e.g., Leonov et al.²⁶) illustrated that material parameters cannot al-

ways be derived in a straightforward manner. This discrepancy is most pronounced for superposition flows. The negative values for G'_{\parallel} also indicate that the difference between parallel and orthogonal superposition moduli cannot be directly translated in material anisotropy during flow.

5. Conclusions

The superposition of small amplitude oscillations on a steady-state shearing motion has been used to study the effect of flow on relaxation mechanisms in complex nonlinear fluids. Parallel superposition data, in particular, have been reported repeatedly for associative polymers. Here, orthogonal and parallel superposition measurements on associative polymers have been compared for the first time. For the HASE system under consideration, as for other nonlinear fluids, the parallel superposition moduli cannot be treated as linear viscoelastic moduli. This is illustrated by the negative values of G'_{\parallel} at low frequencies and the limiting zero-frequency viscosity different from the steady-state viscosity at the same shear rate. On the other hand, orthogonal superposition moduli seem to reflect more clearly the relaxation behavior during flow. The low-frequency data suggest the usual systematic breakdown of the slowest relaxation modes with increasing shear rate. The superposition behavior of associative polymers at higher frequencies deviates from that of normal polymeric or colloidal systems. Both types of superposition indicate an increase of the relaxation modes at intermediate frequencies for associative polymers. This particular response occurs even when no shear thickening is observed in steady shear flow.

For the associative polymers under investigation, the crossover frequency in parallel superposition flow is about an order of magnitude higher than that in orthogonal superposition. Both this phenomenon and the negative G'_{\parallel} values at low frequencies occur in the shear-thinning zone and are caused by the strong coupling of the steady-state flow with the parallel oscillatory flow. Using the crossover frequency or the maximum in G'' value from the parallel superposition measurements, therefore, gives erroneous values for the dominant relaxation times during flow.

It can be concluded that parallel superposition flow is a sensitive technique for qualitatively detecting the effect of flow on the relaxation time in associative polymers under flow. The values for the characteristic times can, however, be off by an order of magnitude. Orthogonal superposition moduli can differ strongly from their parallel counterparts. They can be expected to provide more reliable values of the characteristic times.

Acknowledgment. B.K. thanks the Research Council of the Katholieke Universiteit Leuven for a postdoctoral fellowship. J.V. acknowledges a postdoctoral fellowship of the Fund for Scientific Research-Flanders (FWO-Vlaanderen).

Supporting Information Available: Three figures supplementing the data in Figures 1 and 2 that show the effect of concentration on the steady-state viscosity and the linear viscoelastic moduli of the TT-615 associative polymer. This material is available free of charge via the Internet at <http://pubs.acs.org>.

References and Notes

- Winnik, M. A.; Yekta A. *Curr. Opin. Colloid Interface Sci* **1997**, *2*, 424–436.

- (2) Semenov, A. N.; Joanny, J.-F.; Khokhlov, A. R. *Macromolecules* **1995**, *28*, 1066–1075.
- (3) S      , Y.; Aznar, R.; Porte, G.; Berret, J.-F.; Calvet D.; Collet, A.; Viguier M. *Phys. Rev. Lett.* **1998**, *81*, 5584–5587.
- (4) Pham, Q. T.; Russel, W. B.; Thibault, J. C.; Lau, W. *Macromolecules* **1999**, *32*, 2996–3005.
- (5) Annable, T.; Buscall, R.; Rammile, E.; Whittlestone, D. *J. Rheol.* **1993**, *37*, 695–726.
- (6) Rehage, H.; Hoffmann, H. *Mol. Phys.* **1991**, *74*, 933–973.
- (7) Leibler, L.; Rubinstein, M.; Colby, R. H. *Macromolecules* **1991**, *24*, 4701–4707.
- (8) Tanaka, F.; Edwards S. F. *J. Non-Newtonian Fluid Mech.* **1992**, *43*, 247–271.
- (9) Marrucci, G.; Bhargava, S.; Cooper, S. L. *Macromolecules* **1993**, *26*, 6483–6488.
- (10) Jenkins, R. D.; DeLong, L. M.; Basset, D. R. In *Hydrophilic Polymers*; Glass, J. E., Ed.; ACS Advances in Chemistry Series 248; American Chemical Society: Washington, D.C., 1996; pp 425–447.
- (11) Tirtaatmadja, V.; Tam, K. C.; Jenkins, R. D. *Macromolecules* **1997**, *30*, 1426–1433.
- (12) Tirtaatmadja, V.; Tam, K. C.; Jenkins R. D. *Macromolecules* **1997**, *30*, 3271–3282.
- (13) Jenkins, R. D. The Fundamental Thickening Mechanism of Associative Polymers in Latex Systems: A Rheological Study. Ph.D. Dissertation, Lehigh University, Bethlehem, PA, 1990.
- (14) S      , Y.; Jacobsen, V.; Berret, J.-F.; May, R. *Macromolecules* **2000**, *33*, 1841–1847.
- (15) English, R. J.; Gulati, H. S.; Jenkins, R. D.; Khan, S. A. *J. Rheol.* **1997**, *41*, 427–444.
- (16) Simmons, J. M. *J. Sci. Instrum.* **1966**, *43*, 887–892.
- (17) Mewis, J.; Schoukens, G. *Faraday Discuss. Chem. Soc.* **1978**, *65*, 58.
- (18) Zeegers, J.; Van den Ende, D.; Blom, C.; Altena, E. G.; Beukema G. J.; Mellema, J. *Rheol. Acta* **1995**, *34*, 606–621.
- (19) Walker, L. M.; Vermant, J.; Moldenaers, P.; Mewis, J. *Rheol. Acta* **2000**, *39*, 26–37.
- (20) English, R. J.; Raghavan, S. R.; Jenkins, R. D.; Khan, S. A. *J. Rheol.* **1999**, *43*, 1175–1194.
- (21) Vermant, J.; Walker, L.; Moldenaers, P.; Mewis, J. *J. Non-Newtonian Fluid Mech.* **1998**, *79*, 173–189.
- (22) Tanner, R. I.; Williams, G. *Rheol. Acta* **1971**, *10*, 528–538.
- (23) Yamamoto, M. *Trans. Soc. Rheol.* **1971**, *15*, 331–344.
- (24) Vermant, J.; Moldenaers, P.; Mewis, J.; Ellis, M.; Garritano, R. *Rev. Sci. Instrum.* **1997**, *67*, 4090–4097.
- (25) Booij, H. C. *Rheol. Acta* **1966**, *5*, 215–221.
- (26) Kwon, Y.; Leonov, A. I. *Rheol. Acta* **1993**, *32*, 108–112.
- (27) De Cleyn, G.; Mewis, J. *J. Non-Newtonian Fluid Mech.* **1981**, *9*, 91–105.
- (28) Tanner, R. I.; Simmons, J. M. *Chem. Eng. Sci.* **1967**, *22*, 1803–1815.
- (29) Xu, B.; Yekta, A.; Winnik, M. A. *Langmuir* **1997**, *13*, 6903–6911.
- (30) Frith, W. J.; Strivens, T. A.; Mewis, J. *J. Colloid Interface Sci.* **1990**, *139*, 55–62.
- (31) Witten, T. A.; Cohen, M. H. *Macromolecules* **1985**, *25*, 1915–1920.
- (32) Biebaut G. *Rheology of Colloidal Suspensions: Effects of Stabilizer Layer Thickness*, Ph.D. Thesis, Katholieke Universiteit Leuven, Leuven, Belgium, 1999; pp 192–194.
- (33) Macdonald, I. F. *Trans. Soc. Rheol.* **1973**, *17*, 537–555.
- (34) Markowitz, H. Proceedings of the Fifth International Congress on Rheology; Onogi, S., Ed.; Tokyo University Press: Tokyo, Japan, 1969; pp 499–510.

MA000987P